29 November 2023

Search for Dark photon in reconstructed High Luminosity LHC Monte-Carlo simulated events

Nivedaa Dhandapani

under the guidance of **Dr. Thomas Owen James** and **Dr. Giovanni Petrucciani**

Summary

The High Luminosity (HiLumi) upgrade of the LHC will observe a ten-fold increase in the integrated luminosity of the accelerator which in turn will significantly increase the pile-up and unwanted background events hindering our efforts in the search for new physics. In this project we tried to place cuts on simulated Monte-Carlo data with di-muon final state and analyse the dark photon selection efficiency and acceptance with respect to the given background. We have also tried to visualise the challenges faced in storing high volume data and verify the feasibility of storing data after cuts in high luminosity upgrade. Finally we use a neural network to place cuts in order to improve signal efficiency based on the data used in training and testing.

Contents

1 Introduction

Initially it was thought that new particles beyond the Standard Model(SM) will interact with the visible ordinary SM particles through well established interactions mediated by gauge bosons within this framework. Our inability to discover these particles for the last 50 years and the mounting frustration has led us to challenge this hypothesis. With our hope of a breakthrough waning, there has been a growing interest in seeing these particles as not charged under SM, therefore getting them their name dark particles. Maybe no new particles have been seen simply because they do not interact through the SM gauge interactions.

In order to solve these challenges we turn to electromagnetic and weak interactions and assume that dark and ordinary sectors also interact through a portal. We will focus on the vector portal where the interaction takes place because of the kinetic mixing between one dark and one visible Abelian gauge boson. A search for an unknown particle amidst thousands of processes arising from a single collision can seem daunting, but thanks to the development of several theoretical limits and experimental algorithms we can narrow down where to look for these rare dark photons.

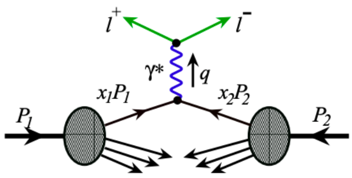

Figure 1: Dark photon mediated production of massive lepton pair

In the LHC, dark photons could be produced in Drell-Yan like process where instead of virtual SM boson mediators we have kinetically mixed dark photon mediating the production of massive lepton pairs (see Figure 1). We will be focusing our efforts on the dimuon channel only and not the dielectron channel since the latter comes with its set of challenges such as higher background levels, tendency of electron to lose significant energy in trackers etc. The very obvious case of background process while looking for our dark photon signal is the SM mediated Drell-Yan. Other backgrounds considered include $J\psi \to \mu^+\mu^-$, $bs \to \mu^+\mu^-$ and production of muons from pile-up collisions.

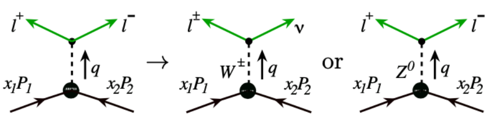

(a) Drell-Yan mediated by SM bosons

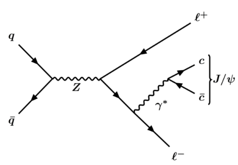

(b) $J\psi \to \mu^+\mu^-$

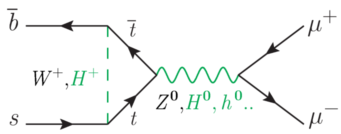

(c) $\bar{b}s \to \mu^+\mu^-$

Figure 2: Feynman Diagrams of Background processes

In the upcoming sections we will go through our methods to improve signal efficiency with respect to the background.

2 Analysis

The project analyses data using the ROOT package (RDataFrame) in python.

2.1 Manual Cuts

Method

The first step in analysing the events is to pair up the muons observed in each event to create muon pairs. Now we define a new set of parameters for each pair of muons derived from the existing set of variables observed for isolated muons. These new parameters include invariant mass, net charge, maximum pseudorapidity (η), minimum transverse momentum (p_T) and difference in initial position along beam axis (Δd_z), all calculated for each muon pair.We also consider hardware variables such as `hwIsoSumAp`, `hwIsoSum` and `hwQual`.

Selection criterion on these variables are manually chosen after observing the distribution of events upon adjustment. The efficacy of the selection criteria is examined through a set of selected performance verifiers.The two criteria finalised for further analysis are as follows:

Cut 1 (Old cut)

1. minimum $p_T > 2$GeV
2. Net charge $< |0.1|$ charge units
3. $\Delta d_z < |1|$ cm
4. maximum $\eta <= |2|$
5. $0.03125 \times$ `hwIsoSumAp` $<= 1.5$ [1]
6. $0.03125 \times$ `hwIsoSum` $<= 1.5$
7. `hwQual` > 75 [2]

Cut 2 (New cut)

1. minimum $p_T > 0.25 \times$ invariant mass
2. Net charge < 0.1 charge units
3. $\Delta d_z < |1|$ cm
4. maximum $\eta <= |2|$
5. $0.03125 \times$ `hwIsoSumAp` $<= 1.5$
6. $0.03125 \times$ `hwIsoSum` $<= 1.5$
7. `hwQual` > 75

The key difference between the two cuts is the chosen threshold of p_T for event selection. In the upcoming subsections we will look at how the cuts improve signal efficiency.

[1]Criterion 5, 6 in both cuts 1 and 2 mean that there should be less than 1.5 GeV of transverse momentum of tracks in a cone around the muon

[2]Criterion 7 (in both cuts) is implemented to reject muons which have signal in only one chamber of the muon system

Results

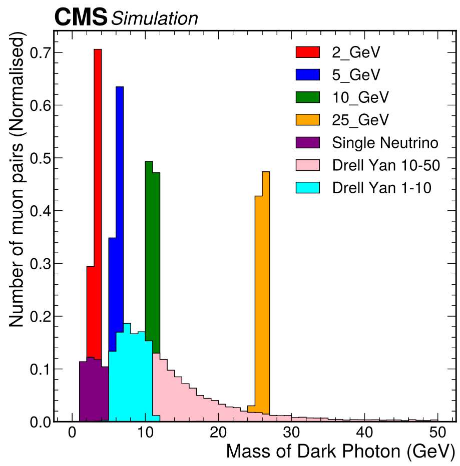

Figure 3: Signal and select background events represented in the same normalised histogram

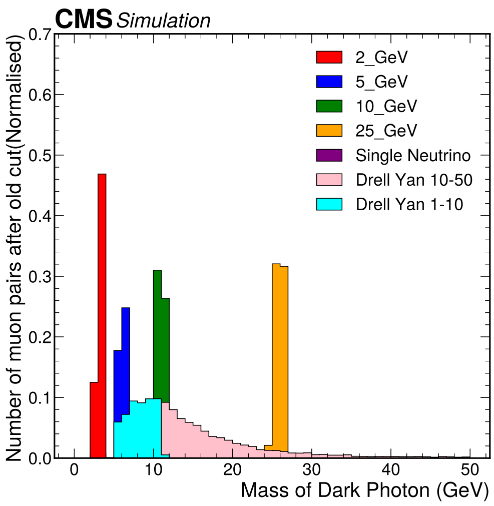

(a) After cut 1

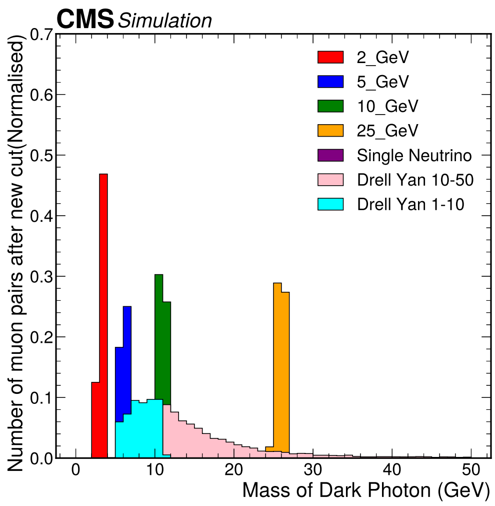

(b) After cut 2

Figure 4: Signal and background after cuts normalised to the total area under Figure 3

The signal strength in Figure 4 has decreased by nearly two-third from in Figure 3, however, the single neutrino gun background seems to be practically non-existent and the number of DY events have also gone down significantly. These plots don't clearly illustrate the differences in the two cuts. This is clearly seen in the log plot of the background events shown in Figure 5. One thing to note here is that all of these events consist of muon pairs which are index matched to their corresponding generated muons (this is not applicable to pure pile-up background).

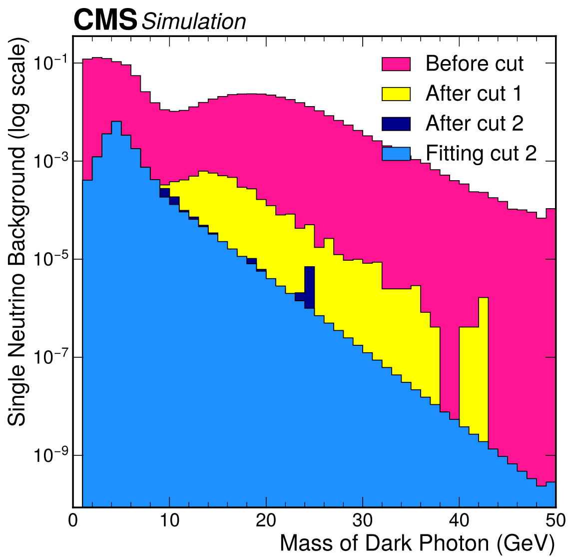

(a) Pure Pile-up [3]

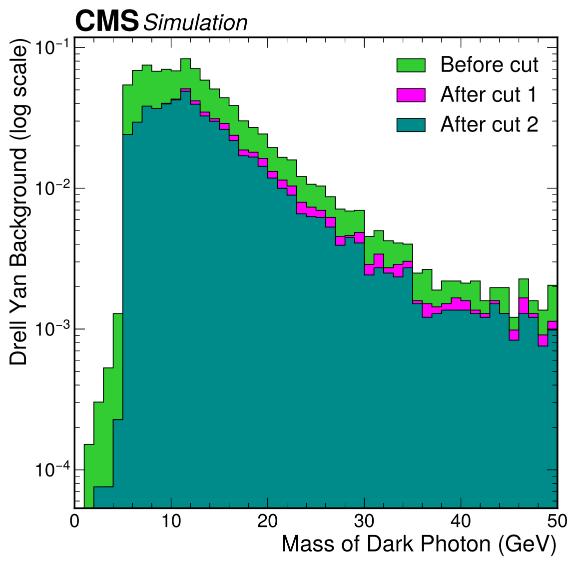

(b) Drell-Yan

Figure 5: Log scale of background events histogram for different cuts

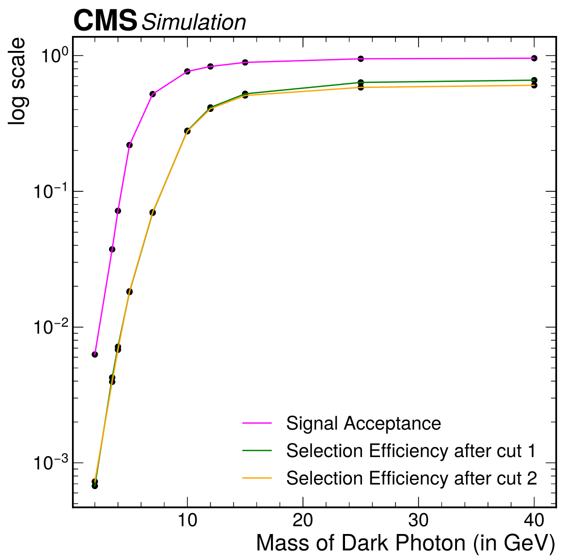

Figure 6: Log scale plot of signal acceptance and selection efficiency for both cuts

Let us define a few metrics which will help us quantify this difference better: **signal acceptance** is defined as the ratio of muon pairs which are index matched to their corresponding generated muons to the total number of muon pairs. **Selection efficiency** is

[3]In this plot, `fitting cut 2` is a smoothed version of `after cut 2` where the tail of the distribution is replaced with an exponential fitted from the `after cut 2` histogram

defined as the ratio of index matched muon pairs that pass through the selection criteria to the total number of muon pairs. By this definition we will have different selection efficiencies corresponding to each new selection criterion.

The plots of signal acceptance and selection efficiencies corresponding to cut 1 and cut 2 for various projected dark photon mass signals are shown in Figure 6. There isn't much difference between cut 1 and cut 2 with respect to efficiency which is encouraging since we observe that tightening the cut has only resulted in minor loss in efficiency .

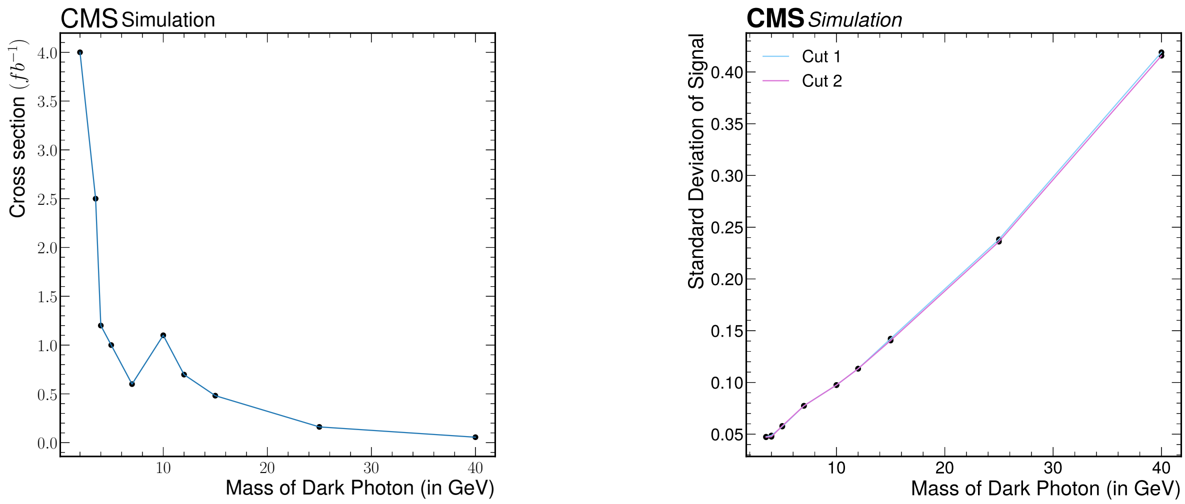

(a) Cross section used for various dark photon mass signals for $\epsilon^2 = 3 \times 10^{-6}$

(b) Standard deviation upon fitting histogram

Figure 7: Quantities used to calculate sensitivity

In the hopes of distinguishing the two cut in terms of their performance we introduce a quantity *sensitivity* of the signal which is defined as the ratio between the expected signal event yield and the statistical uncertainty on the background event yield in a region around the signal mass peak. This is expressed as:

$$\frac{N_s}{\sqrt{N_b}} = \frac{N_s}{\sqrt{(\Delta N_b/\Delta m) \times 2\sigma_{\text{Gauss}}}} \tag{1}$$

where

- N_s = (Area under di-muon histogram of a signal after the cut)$\times$Cross section(σ_{cross})$\times$ Luminosity (L)
- N_b is the quantity above but for all background.
- Δm is the bin width of the histogram.
- σ_{Gauss} is the standard deviation obtained after fitting a Gaussian curve on the signal (as shown in 7(b)).

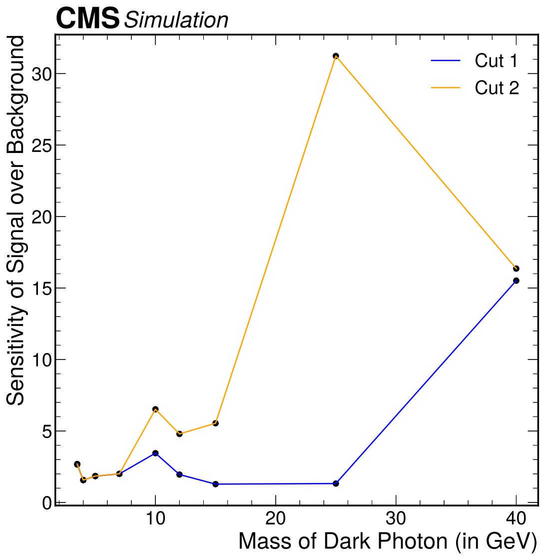

Figure 8: Sensitivity of dark photon signal for different simulated masses

Result

The sensitivity of the signal for different dark photon masses is shown in Figure 8. We can see a very clear distinction between the two cuts and cut 2 is superior to cut 1 since it has a greater sensitivity.

Despite this exercise we observe agree that manual cuts are not the most rigorous method of signal isolation. In the next section we will introduce a powerful method which will place the cuts based on data.

2.2 Neural Networks

Construction

```
model = Sequential([tf.keras.layers.Dense(32,activation = "gelu",input_shape=(14,),name = "hd1"),
                    tf.keras.layers.Dropout(0.2),
                    tf.keras.layers.Dense(32,activation = "gelu"),
                    tf.keras.layers.Dropout(0.2),
                    tf.keras.layers.Dense(32,activation = "gelu"),
                    tf.keras.layers.Dense(1,activation = "sigmoid")])


opt          = Adam(learning_rate=1e-3)
losses       = tf.keras.losses.BinaryCrossentropy()
device = 0
n_epochs = 100
```

Figure 9: NN used

The Neural Network (Figure 9) used is built with `tensorflow.keras` package in python. The network has three hidden layers with 32 hidden units each. The three hidden layers use `gelu` activation while the output layer uses `sigmoid` activation function. The learning rate α is chosen as 10^{-3}.

The neural network was given a randomised half of signal and background events as training dataset. We feed all four backgrounds mention in the introduction to the NN to be trained on. We now plot the ROC curves for testing data for signals of different dark photon masses.

Result

We can clearly observe the AUC of ROC (Figure 10) increases with increasing mass which implies that our NN is able to tell background from signal with higher accuracy as mass of dark photon signal increases.

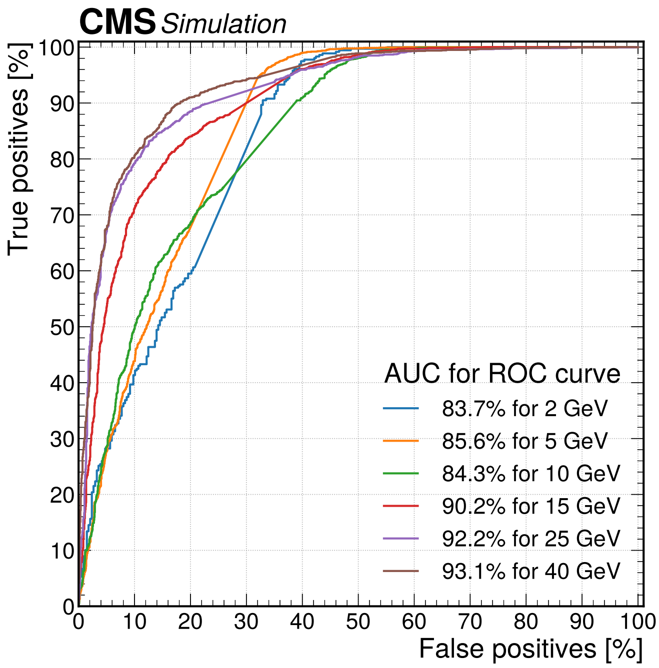

Figure 10: ROC curve of dark photon signal for different simulated masses

2.3 Data Rate Analysis

This subsection aims to check if the current infrastructure can comfortably accommodate the increase in data storage needs expected from the high luminosity upgrade of the LHC.

Each muon takes 96 bits of storage. We calculate the rates of data flow by taking two frequencies of bunch crossing (i.e.,) 40 MHz and 31.5 MHz[4]. So the rate of data received in bits per second is given by

$$\text{data rate (in bits)} = \text{Number of muons} \times 96 \text{ bits} \times 31.5 \text{ MHz}$$

[4]This frequency is to account for the fact that not all LHC bunches are filled and so the collision rate is less than 40 MHz

An orbit of data has 3564 events and for each event there is 64 bits of extra overhead data that needs to be considered. The average data per orbit in bits is

$$\text{Average data per orbit (in bits)} = 3564 \times [(\text{average number of muons} \times 96 \text{ bits}) + 64 \text{ bits}].$$

The maximum number of muons recorded is 12 which is in turn used to calculate the upper limit of data rate in bps and in Gbps. This data is split into 18 parts and is sent in through the nodes into the DTH [5]. This gives:

$$\text{data rate in DTH} = 18 \times \text{data rate per node}$$

The LHC collects data for a total of $5.35 \times 10^6 s$ in a year

Results

Putting together all the information from the previous subsection we get

- Average data rate per node at 31.5 MHz is 306.90 Mb/s.
- Average data rate in DTH at 31.5 MHz is 5.52 Gb/s.
- Total data size per year at 31.5 MHz is 3.53 PB.
- The average size for one orbit (3564 events) is 83.90 kB.
- For a realistic LHC filling scheme with 2800 colliding bunches, the average size for one orbit is 65.90 kB.

The results agree with our expectations and can therefore be supported by the current storage infrastructure at LHC.

3 Conclusion

In this project we placed cuts of various strengths and observed that despite tightening the cut (cut 2), the selection efficiency falls slightly in comparison to a more lenient cut (cut 1). We also established that sensitivity to signal increases with dark photon mass and that sensitivity is greater for tighter cut across higher mass ranges (> 5 GeV) while remaining almost same for both cuts at lower masses.

Upon training NN to select signal out of the background we observe that it's performance is significantly higher for larger dark photon masses. We could train the NN on more data sets which can improve the selection efficiency making our findings more robust. We can try to implement this NN onto an FPGA upon increasing it's efficiency which is a scope for future research on this project.

After performing rate analysis, we conclude that the amount of the data expected to be received during the HL run can be supported by the storage infrastructure at LHC.

4 Acknowledgements

I would like to express my heartfelt gratitude to my supervisors, Dr. Giovanni Petrucciani and Dr. Thomas Owen James for their continued unwavering support and guidance through every step of my project. Their nuanced insights and incredible mentorship has taught me so much about what it means to do research at CERN. I would also like to thank Rocco Ardino for his help throughout this project.

I would like to acknowledge the contributions of Diptarko Choudhury (NN) and Pietro Cappelli (rate analysis). I learnt a lot from having discussions with them and their feedback added great value on my journey.

I would also like to acknowledge the Summer student team of CERN (Barbara Binder and Ana Dordevic) for their organisational efforts and timely assistance, making this an unforgettable experience.

Finally, I would like to thank my partner Madhu for supporting me, always.

Bibliography

[1] B. Holdom., (1986) *Two U(1)'s and ϵ charge shifts. Phys. Lett. B*, **Volume 166** 196–198. DOI: 10.1016/0370-2693(86)91377-8

[2] ATLAS Collaboration, (2012). *Search for the decay $B_s^0 \to \mu^+\mu^-$ with the ATLAS detector*, *Phys. Lett. B*, **Volume 713**, 387–407. DOI: 10.1016/j.physletb.2012.06.013

[3] J. Peng, et al., (2016). *The Drell-Yan Process.*,*The Universe*, **Volume 4**(Issue No. 3), 34–37. Link: https://inspirehep.net/files/ce4c857d3b2e3642c4ff2bde4e67c775

[4] M. Fabbrichesi, et al., (2020). *The dark photon.* DOI: arXiv:2005.01515v3 [hep-ph]

[5] V. Amoiridis, et al., (2022). *CMS phase-2 DAQ and timing hub prototyping results and perspectives.*, *Journal of Instrumentation*, **Volume 17**, 2–4. DOI: 10.1088/1748-0221/17/05/C05003